Latin American Journal of Solids and Structures
www.lajss.org

Effect of blast loading on CFRP-Retrofitted RC columns – a numerical study

Abstract

This study aims to investigate the effect of blast loads generated as a result of explosive charges on the existing exterior RC circular columns of a typical building in the city of Riyadh. A procedure has been developed for evaluating the dynamic characteristics of the circular column with and without retrofitting. A wide range of parametric studies have been performed as part of this investigation to examine the effects of stand-off distance, charge weight and the presence of CFRP retrofitting on the level of damage to the RC column. The nonlinear finite element analysis was carried out using LS-DYNA software with explicit time integration algorithms. Different charge weights of 100, 200, 500 and 1000 kg equivalent weight of TNT at stand-off distances of 1, 4 and 15 m were considered. Results described in this paper indicate that CFRP strengthening could be an effective solution to limit the damage caused by moderate explosions. The stand-off distance was found to play a very important role in mitigating the adverse effects of a blast. The results also indicate that the maximum lateral deflection experienced by the column decreased exponentially with the increase in the stand-off distance and also decreased for the columns strengthened with CFRP, compared with the unstrengthened columns.

Keywords

blast loads, LS-DYNA, Finite element models, RC Columns, CFRP strengthening .

H.M. Elsanadedy, T.H. Almusallam, H. Abbas*, Y.A. Al-Salloum and S.H. Alsayed

Specialty Units for Safety and Preservation of Structures, College of Engineering, King Saud University, Riyadh 11421 – Saudi Arabia

Received 1 Oct 2010;
In revised form 9 Feb 2011

* Author email: abbas_husain@hotmail.com

1 INTRODUCTION

In the recent past, structures all over the world have become susceptible to the threat of terrorist attacks, accidental explosions and other unthought-of explosion related failures. Buildings and critical infrastructure vulnerable to explosions include government buildings, embassies, financial institutions, densely populated commercial structures, and other buildings of national heritage or landmarks. Consequently, a number of concerns have been raised on the vulnerability and behavior of these structures under extreme loadings.

In a study carried out by Lan *et al.* [14], design techniques for reinforced concrete (RC) columns which are capable of protecting them from the effects of close-in detonation of a suitcase bomb have been described. LS-DYNA software [15] was used for the finite element analysis of column using solid elements for concrete and beam elements for reinforcing bars. The elements were allowed to erode at a principal tensile strain of 50%. It was shown that the tie spacing plays an important role in the post-blast residual load capacity of columns. Buchan and Chen [6] presented a state-of-the-art review on retrofitting concrete and masonry structures by FRP composites for blast protection. The advantages of FRP and polymer retrofitting in increasing its strength and ductility and reducing fragmentation were highlighted.

Muszynski *et al.* [20, 21] reported results from explosion experiments on RC columns strengthened with GFRP and CFRP. However, during the tests, a previously tested wall became detached and collided with the retrofitted columns, shearing the top and the bottom. The reason for the spoiled tests was a higher than predicted pressure from the explosive.

Crawford *et al.* [9] conducted experiments for studying the blast vulnerability of a 350mm square column of a four story office building. The column failed mainly in shear and the rupture of longitudinal rebars accounted for the majority of the displacement. An identical column was retrofitted with six layers of horizontal CFRP wraps for shear enhancement and three vertical layers for flexural enhancement. The retrofitted column under the same blast loading appeared to be elastic with no permanent noticeable deformation. The static load testing of identical columns was found useful in simulating the blast tests.

Crawford *et al.* [11] conducted numerical analyses of 1.10 m diameter circular RC column from a multi-story building retrofitted with CFRP composites to determine its vulnerability to terrorist attacks. DYNA3D, a lagrangian FE code, was used to assess the performance of the column against 682 and 1364 kg TNT charges at 3.05, 6.1 and 12.2 m stand-off distances. Modeling challenges highlighted were the effect of confinement on the concrete strength and ductility, strain rate effects, direct shear response and determining loading on many structural members. An explosive loading was applied and a pressure at the top of the column was used to simulate the upper stories. The concrete volume was modeled with 8-node brick elements; reinforcement bars were represented with truss elements and shell elements were used for the floors and joists. All results showed that composite retrofits could have a beneficial effect on the performance of the columns and therefore prevent progressive collapse. The retrofitting was shown to reduce the lateral displacement considerably.

In addition to 3D finite element models, single degree of freedom (SDOF) models [9, 10, 19] have also been used to predict the response of FRP-retrofitted columns against blast loads. The predictions from such simple models were close to the observed displacement from the explosive tests. Malhotra *et al.* [16] give a good overview of the method. Although these simplified methods are quite useful, three-dimensional analysis, in contrast, provides a more in-depth understanding by incorporating all aspects of the response of concrete structures subjected to blast effects.

Riisgaard *et al.* [22] presented experimental and numerical results of two polymer reinforced compact reinforced concrete (PCRC) columns subjected to close-in detonation. PCRC is a fiber

reinforced densified small particle system (FDSP) combined with a high strength longitudinal flexural rebar arrangement laced together in the out of plane direction, using polymer lacing to avoid shock initiated disintegration of the structural element. The two columns were subjected to 7.6 kg of Penta-Erythritol Tri-Nitrate (PETN) HE (85/15) at a stand-off distance of 0.4 m. For both the columns, the concrete matrix was damaged and both columns suffered from bending failure. The amount of aramid lacing was found to have a positive effect on the performance.

Shi *et al.* [23] proposed a numerical method to generate pressure–impulse diagram for RC column and developed analytical formulae for its development. Parametric studies were also carried out to investigate the effects of geometric and material characteristics. In another study, Shi *et al.* [24] modeled the bond slip between rebar and concrete using one-dimensional slide line contact model in LS-DYNA. The parameters of the one-dimensional slide line model were derived from common pullout test data. A comparison of numerical results is made with experimental data. A case study was also carried out to investigate the bond-slip effect on numerical analysis of blast-induced responses of a RC column.

Bao and Li [4] used LS-DYNA to provide numerical simulations of the dynamic responses and residual axial strength of reinforced concrete columns subjected to short stand-off blast conditions. The model is verified through correlated experimental studies. The effects of transverse reinforcement ratio, axial load ratio, longitudinal reinforcement ratio, and column aspect ratio were studied through parametric studies. A formula was proposed for estimating the residual axial capacity based on the mid-height displacement.

King *et al.* [12] discussed typical building retrofit strategies for load bearing and non-load bearing structural members through strengthening, shielding, or controlling hazardous debris. El-Dakhakhni *et al.* [26] developed a nonlinear strain rate dependent model to study the response of blast-loaded reinforced concrete columns. The moment-curvature relationships and force-moment interaction diagrams were used for the development of pressure-impulse diagrams. The uncertainties associated with RC column reinforcement details and possible increase of column axial load was also incorporated. Berger *et al.* [5] performed blast testing on scaled reinforced concrete columns to study the behaviour of different types of strengthening of Steel Reinforced Polymer (SRP), CFRP and SRP/CFRP hybrid combination. It was observed that the SRP-strengthened columns were quite similar to those strengthened with CFRP. The SRP was found to be an effective external strengthening material for increasing the resistance of concrete components, providing similar performance to CFRP wraps at potentially lower cost.

It is seen that the research carried out in the area is mostly qualitative and the behavior of FRP-strengthened structures under blast loading is not well understood and no proper design guidelines are available. The lack of understanding is primarily due to the complexity of the problem where too many variables exist and experiments alone do not lead to effective design methods. Instead, an in-depth understanding of the structural behavior and accurate modeling of the dynamics of the structure under blast waves is required. In order to assess the possibility of progressive collapse of the building, it is extremely important to study the effects of blast

loadings on the columns of the structure independently. The present study aims to analyze a RC circular column for investigating the role of CFRP in improving the collapse behavior thus avoiding the progressive collapse. The study considers different charge weights at varying stand-off distances. The RC circular column considered for the present study was selected from a real building located in Riyadh. A close inspection of the building premises revealed that the stand-off distance was virtually zero, which allowed the placement of explosive at a minimum stand-off distance of 1 m.

2 DYNAMIC CHARACTERISTICS OF COLUMN

The column selected for the study is a typical circular column of 600 mm diameter and 4 m high. The column is reinforced with 16ϕ16 longitudinal bars and ϕ10@200 mm c/c as ties. The concrete grade of the column is taken as M30. The clear concrete cover to the ties is taken as 30 mm, as shown in Fig. 1. The column represents a real life column of one of the reinforced concrete structures in Riyadh.

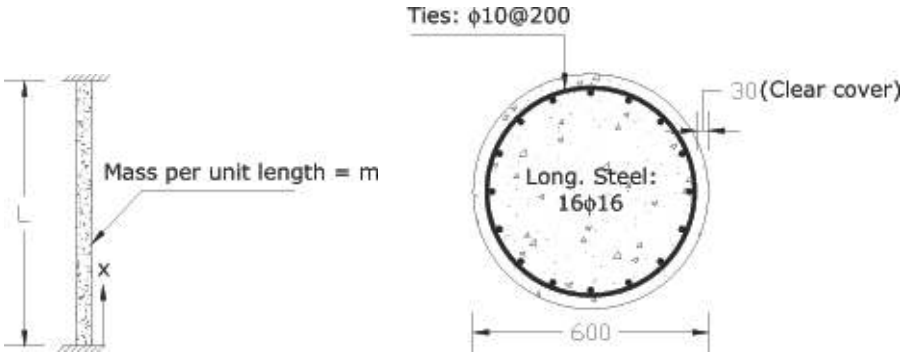

(a) Column (b) Column cross-section

Figure 1 Cross-section for the RC column with reinforcing bars (All dimensions are in mm).

The effect of strengthening has been studied numerically by retrofitting the column with CFRP layers of 1 mm thickness per layer. Two layers of CFRP were thus applied as hoops for enhancement of shear strength and concrete confinement and two layers were provided along the length of the column to increase its flexural capacity. The properties of materials used are given in Table 1.

2.1 Section properties

Considering a circular reinforced concrete column section of radius r and reinforced with n longitudinal steel bars of diameter ϕ (area of steel = A_{st}) as shown in Fig. 2. The section has been retrofitted for flexural as well as shear strengthening with externally bonded layers of CFRP along the longitudinal direction (thickness = t_f) and along circumferential direction (thickness = t_{fs}) respectively.

Table 1 Material properties used in the analysis.

Concrete [1, 2]	
Material Model	Type 072R3 (Karagozian & Case Model)
Uni-axial compressive strength (MPa)	30
Uni-axial tensile strength (MPa)	3.0
Poisson's Ratio	0.2
Reinforcing Steel	
Material Model	Type 024 (Elasto-Plastic model)
Modulus of Elasticity (MPa)	200,000
Poisson's Ratio	0.3
Yield Stress (MPa)	500
Failure Strain	0.1
CFRP	
Material Model	Type-054-055 (Enhanced Composite Damage model)
Thickness of each layer (mm)	1.0
Young's Modulus in Long. Dir. (MPa)	82000
Young's Modulus in Transverse Dir. (MPa)	8200
Poisson's Ratio	0.25
Longitudinal Tensile Strength (MPa)	834
Transverse Tensile Strength (MPa)	83.4

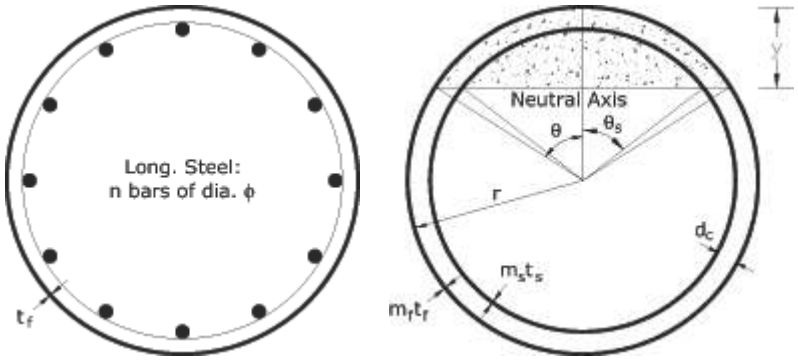

(a) Retrofitted column section (b) Cracked transformed section

Figure 2 Cross-section of RC column considered in analysis.

The properties of the gross transformed section are given by:

$$A_g = \pi r^2 + (m_s - 1)\, A_{st} + 2\pi m_f r t_f \tag{1}$$

$$I_g = \frac{\pi}{4} r^4 + \pi\,(m_s - 1)\, r_s^3 t_s + \pi m_f r^3 t_f \tag{2}$$

where,

A_g gross transformed area of cross-section,

I_g moment of inertia of gross transformed section,

r_s radius of equivalent smeared ring for longitudinal steel,
$r_s = r - d_c - \dfrac{\phi}{2}$

d_c clear cover to longitudinal reinforcing bars,

t_s thickness of equivalent smeared ring for longitudinal steel,
$t_s = \dfrac{n\phi^2}{8r_s}$

m_s modular ratio of reinforcing steel,
$m_s = \dfrac{E_s}{E_c}$

m_f modular ratio of CFRP,
$m_f = \dfrac{E_f}{E_c}$

The depth of neutral axis (NA) of the section may be found by taking the moment of effective transformed areas about NA, thus giving:

$$A_c y_c + A_{esc} y_{sc} + A_{efc} y_{fc} - A_{est} y_{st} - A_{eft} y_{ft} = 0 \tag{3}$$

where,

A_c area of concrete in compression,
$A_c = r^2\,\{\theta - \sin(\theta)\cos(\theta)\}$

y_c distance of centroid of the area of concrete in compression from NA,
$y_c = \dfrac{2r}{3}\left\{\dfrac{\sin^3(\theta)}{\theta - \sin(\theta)\cos(\theta)}\right\} - r + y, \quad \theta = \cos^{-1}\left(\frac{r-y}{r}\right)$

A_{esc} area of smeared ring of steel in compression,
$A_{esc} = 2\,(m_s - 1)\, r_s \theta_s t_s$

y_{sc} distance of centroid of the smeared ring of steel in compression from NA,
$y_{sc} = 2r_s^2 \sin(\theta_s) - r + y$

A_{est} area of smeared ring of steel in tension,
$A_{est} = 2 m_s r_s\,(\pi - \theta_s)\, t_s$

y_{st} distance of centroid of the smeared ring of steel in tension from NA,
$y_{st} = 2r_s^2 \sin(\pi - \theta_s) + r - y$

A_{efc} transformed area of CFRP in compression,
$A_{efc} = 2 m_f r \theta t_f$

y_{fc} distance of centroid of the CFRP in compression from NA,
$y_{fc} = 2r^2 \sin(\theta) - r + y$
A_{eft} transformed area of CFRP in tension,
$A_{eft} = 2m_f r(\pi - \theta) t_f$
y_{ft} distance of centroid of the CFRP in tension from NA,
$y_{ft} = 2r^2 \sin(\pi - \theta) + r - y$

The cracked moment of inertia of the section is given by:

$$I_{cr} = \frac{r^4}{4}\left\{\theta - \sin(\theta)\cos(\theta) + 2\sin^3(\theta)\cos(\theta)\right\} - A_c y_c^2 + (m_s - 1) r_s^3 t_s \{\theta_s + \sin(\theta_s)\cos(\theta_s)\} - A_{esc} y_{sc}^2 + m_s r_s^3 t_s \{\pi - \theta_s - \sin(\theta_s)\cos(\theta_s)\} - A_{est} y_{st}^2 + m_f r^3 t_f \{\theta + \sin(\theta)\cos(\theta)\} - A_{efc} y_{fc}^2 + m_f r^3 t_f \{\pi - \theta - \sin(\theta)\cos(\theta)\} - A_{eft} y_{ft}^2 \quad (4)$$

where, $\theta_s = \cos^{-1}\left(\frac{r-y}{r_s}\right)$.

2.2 Dynamic response

Considering a reinforced concrete column of length L and mass per unit length m, as shown in Fig. 2. The mode shapes of vibration of an Euler column may be expressed as [8]:

$$\phi(x) = A_1 \cos(ax) + A_2 \sin(ax) + A_3 \cosh(ax) + A_4 \sinh(ax) \quad (5)$$

with the first and second spatial derivatives given by:

$$\phi'(x) = \frac{1}{a}\{-A_1 \sin(ax) + A_2 \cos(ax) + A_3 \sinh(ax) + A_4 \cosh(ax)\} \quad (6)$$

$$\phi''(x) = \frac{1}{a^2}\{-A_1 \cos(ax) - A_2 \sin(ax) + A_3 \cosh(ax) + A_4 \sinh(ax)\} \quad (7)$$

where,
x distance measured from one end of column,
a eigen value parameter (unit: Length^{-1}) such that,
$a^4 = \frac{4\pi^2 f^2 m}{EI}$
f natural frequency of column,
m mass per unit length of column
$m = \pi r^2 \rho_c$
r_c density of reinforced concrete,
E_c modulus **of** elasticity of reinforced concrete,
$E_c = 4700\sqrt{f_c}$ [3],
f_c compressive cylinder strength of concrete,
I moment of inertia of column.

In the beginning, when both ends of the columns are fixed i.e. $\phi(c) = \phi'(x) = 0$ at $x = 0$ and at $x = L$, thus giving:

$$\begin{bmatrix} 1 & 0 & 1 & 0 \\ 0 & 1 & 0 & 1 \\ \cos(aL) & \sin(aL) & \cosh(aL) & \sinh(aL) \\ -\sin(aL) & \cos(aL) & \sinh(aL) & \cosh(aL) \end{bmatrix} \begin{Bmatrix} A_1 \\ A_2 \\ A_3 \\ A_4 \end{Bmatrix} = \begin{Bmatrix} 0 \\ 0 \\ 0 \\ 0 \end{Bmatrix} \tag{8}$$

Thus giving the characteristic equation as,

$$\cos(aL)\cosh(aL) = 1 \tag{9}$$

The mass of the column being distributed along the length, there are infinite sets of frequencies and associated modes that satisfy the above equation. The first few values are: $aL = 4.7300$, 7.8532, 10.9956, 14.1372, 17.2788 ...

When the column is subjected to blast, plastic hinges may be formed at the ends thus the boundary conditions get transformed to: $\phi(x) = \phi''(x) = 0$ at $x = 0$ and at $x = L$, thus giving

$$\begin{bmatrix} 1 & 0 & 1 & 0 \\ -1 & 0 & 1 & 0 \\ \cos(aL) & \sin(aL) & \cosh(aL) & \sinh(aL) \\ -\cos(aL) & -\sin(aL) & \cosh(aL) & \sinh(aL) \end{bmatrix} \begin{Bmatrix} A_1 \\ A_2 \\ A_3 \\ A_4 \end{Bmatrix} = \begin{Bmatrix} 0 \\ 0 \\ 0 \\ 0 \end{Bmatrix} \tag{10}$$

The characteristic equation obtained for the above is:

$$\sin(aL)\sinh(aL) = 0 \tag{11}$$

The roots of the above equation are: $aL = n\pi$, where, $n = 1, 2, 3, \ldots$.

It may be noted here that the above analysis is based on the assumption of prismatic column section and perfectly straight column axis. The exposure of column to blast may result in non-uniform material erosion, permanent deformation in the column axis and the hinge action as a result of damage may not occur at both ends or may be partial. It is due to these reasons that the actual response of the column may differ from the analysis presented above.

2.3 Discussion

The section properties of the column taken in the study are given in Table 2. The fundamental frequency and time period calculated based on these section properties and for the two end conditions (i.e. both ends fixed and both ends hinged) are given in Table 3. It may be noted here that the section is considered to be prismatic. The variation in the natural frequency and time period of the column has been plotted in Figs. 3 and 4 respectively.

It is observed from Table 2 that the spalling of cover, which is going to occur due to the vibrations during the blast loading, reduces the cracked moment of inertia of the section by 25.2%. It is assumed that the concrete cover remains attached even after its spalling thus the mass per unit length, which is taken to be uniform, remains unaffected. The advantages of

providing CFRP (longitudinal and circumferential) are two folds – one of increasing the section parameters (area and moment of inertia) and the other of preventing the spalling of concrete cover by providing confinement. The concrete cover which is otherwise brittle because of non-confinement becomes confined and adds to the ductility of the section. The provision of CFRP enhances the cracked moment of inertia of the section by 34.6%. Further, if a comparison is made with the moment of inertia of the section without cover then the enhancement is 79.9%.

Table 2 Section properties of column section.

S. No.	Property	Value
1.	Radius, r (m)	0.3
2.	Concrete grade, f_c (MPa)	30
3.	Reinforcement:	
	Longitudinal	$16\phi16$ ($A_{st} = 32.17\text{cm}^2$, 1.14%)
	Ties	$\phi10$@200
4.	Retrofitting using CFRP	
	Longitudinal	2 layers of 1 mm each
	Hoop	2 layers of 1 mm each
5.	Gross transformed area, A_g (cm^2)	
	no retrofitting	3077.4
	with retrofitting	3197.4
6.	Gross moment of inertia, I_g (m^4)	
	no retrofitting with cover	0.007053
	with retrofitting	0.007594
7.	Depth of NA of cracked section, y (mm)	
	no retrofitting	
	with cover	155.1
	without cover	146.2
	with retrofitting	172.8
8.	Cracked moment of inertia, I_{cr} (m^4)	
	no retrofitting	
	with cover	0.002373
	without cover	0.001776
	with retrofitting	0.003195

It is observed from Table 3 and Figs. 3 and 4 that the change in the values of moment of inertia of the section results in significant change in the natural frequency of different modes of the column.

Table 3 Fundamental time period and frequency of different modes.

State of section	Mode-1		Mode-2		Mode-3		Mode-4	
	T (ms)	f (Hz)	T (ms)	f (Hz)	T (ms)	f (Hz)	T (ms)	f (Hz)
Both ends fixed								
No cracking								
no retrofitting	8.7	115	3.2	317	1.6	622	1.0	1028
with retrofitting	8.4	119	3.0	329	1.5	645	0.9	1067
Cracked section								
with cover	15.0	67	5.4	184	2.8	361	1.7	596
no retrofitting								
without cover	17.0	59	6.2	163	3.1	319	1.9	527
with retrofitting	12.9	77	4.7	214	2.4	419	1.4	692
Both ends hinged								
No cracking								
no retrofitting	19.7	51	4.9	203	2.2	457	1.2	813
with retrofitting	19.0	52	4.7	211	2.1	474	1.2	843
Cracked section								
no retrofitting								
with cover	34.0	29	8.5	118	3.8	265	2.1	471
without cover	38.4	26	9.6	104	4.3	234	2.4	416
with retrofitting	29.3	34	7.3	137	3.3	308	1.8	547

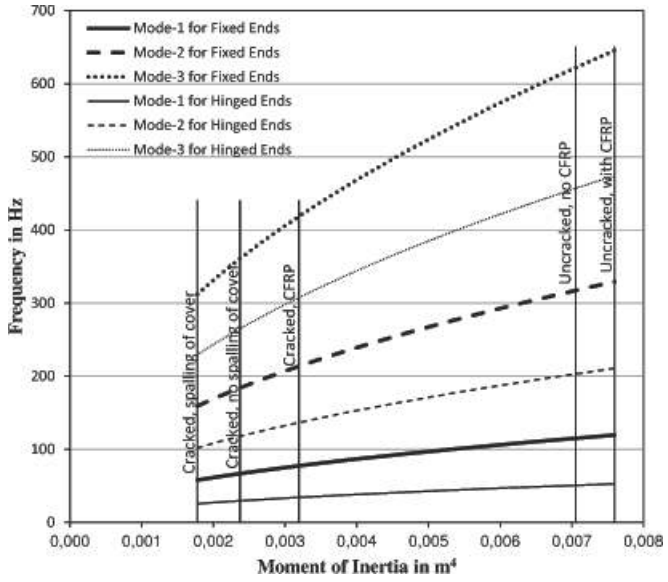

Figure 3 Variation in frequency of different modes for moment of inertia varying from cracked to uncracked section.

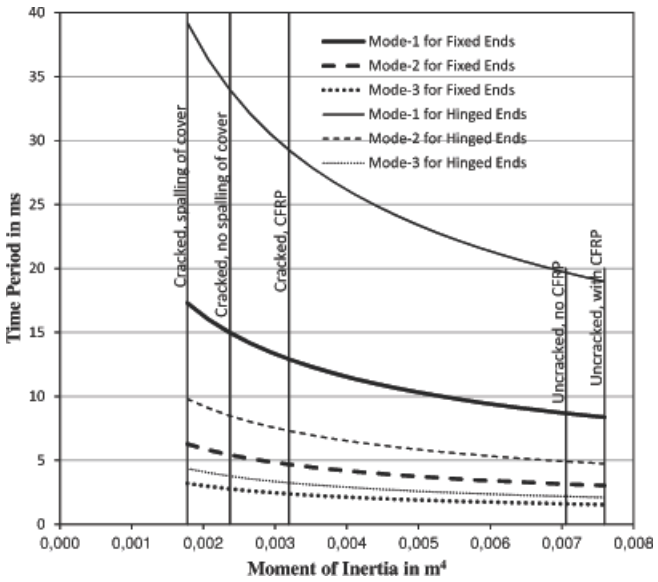

Figure 4 Variation in time period of different modes for moment of inertia varying from cracked to uncracked section.

3 NUMERICAL MODELING

LS-DYNA [15], a general purpose finite element program was used to develop the 3-D model of the column. Two cases were considered in the modeling of the column. The first case involved the column to be modeled without any strengthening and the second case involved strengthening of the column with Carbon Fiber Reinforced Polymer (CFRP) sheets. Damping has been ignored, as it has a negligible effect for short duration, impulsive loads.

3.1 Finite element mesh

Modeling of the column was first completed using ANSYS-Version 11 as it has a very strong graphical user interface and the file was then imported to FEMB (which is a preprocessor for LS-DYNA) database for incorporating the different parts as well as the blast interface and contact segments. A combination of eight and six node solid elements was used to model the concrete volume. The longitudinal reinforcing bars and ties were modeled using 2-node Hughes Lui beam elements. For the modeling of CFRP sheets, 4-node shell elements were employed. Perfect bond was assumed between rebar elements and the surrounding concrete volume and also between the FRP and the concrete substrate. Figure 5 details the mesh discretization for the concrete elements, the CFRP elements and the reinforcing cage used in the study. In order to study the effect of refining the mesh on the numerical results, another fine mesh was created as shown in Table 4. A comparison of the two meshes used in the study is also detailed in the table. The main difference between the two meshes is in the number of concrete elements per column section. The total numbers of elements in the model are 13472 and 18592 for Mesh 1 and Mesh 2 respectively.



(a) Concrete solid elements (b) CFRP shell elements (c) Reinforcing beam elements

Figure 5 Mesh discretization of column in LS-DYNA.

3.2 Material modeling

The Karagozian & Case (K&C) model [17], designated as Material type 072R3 in LSDYNA, was employed to represent concrete for the column. The model is specially designed for predicting the response of concrete under blast loads. It is a three-invariant model which uses three shear failure surfaces and includes damage and strain rate effects. It also incorporates many important features of concrete behavior such as tensile fracture energy, shear dilation and effects of confinement. The reinforcement was modeled using material type 024 to model the elasto-plastic response with strain rate dependency. In order to model the CFRP material, type 054-055 was utilized, which is capable of defining orthotropic material characteristics. The material angles for the longitudinal and circumferential layers were specified as 0° and 90° respectively. The manufacturer's data sheet for the CFRP material was used for defining different material parameters. The laminated shell theory was used for the purpose of correcting the assumption of a uniform constant shear strain throughout the thickness of the composite shell, thus avoiding very stiff results. The failure criteria of composite material used in the analysis is the one proposed by Chang and Chang [7] with special features of compression failure governed by the criteria of Matzenmiller and Schweizerhof [18]. A summary of material properties used in the analysis are presented in Table 1.

3.3 Erosion

The erosion option provides a way of including failure to the material models. This is not a material or physics-based property; however, it lends a great means to imitate concrete spalling phenomena and produce graphical plots which are more realistic representations of the actual events. By activating this feature, the eroded solid element is physically separated from the rest of the mesh. This erosion model represents a numerical remedy to distortion, which can cause

Table 4 Comparison between finite element meshes used in this study.

Parameter	Mesh 1	Mesh 2
Finite element mesh of column section	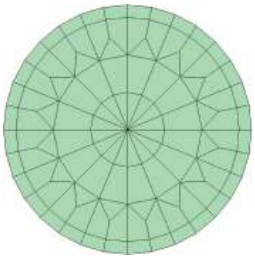	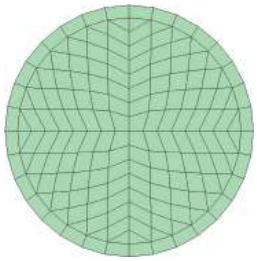
No. of concrete elements per section	112	176
Total No. of concrete elements	8960	14080
Size of concrete element	ranges from 30 to 90 mm	ranges from 30 to 50 mm
No. of beam elements for longitudinal bars	1280	1280
Length of longitudinal bar element	50 mm	50 mm
No. of beam elements for transverse ties	672	672
Length of transverse tie element	50 mm	50 mm
No. of FRP shell elements	2560	2560
Size of FRP shell element	50 × 59 mm	50 × 59 mm
Total No. of elements per model	13472	18592

excessive and unrealistic deformation of the mesh. The application of erosion to the simulated model requires calibration with experimental results; however in the absence of experimental validation, the consequence of possible discrepancy in the erosion specified is limited. This is because the damage level of the concrete material is basically governed by the material model itself. In this study, the concrete elements in the RC column were allowed to erode when the principle tensile strain reached 50% [14]. Column failure is characterized by the volume of eroded concrete elements within a particular section with respect to the total elements in the section, which will have an index about the axial load resistance of the column.

3.4 Loading and boundary conditions

Fixed boundary conditions were assigned for the top and bottom nodes of the column. The axial load acting upon the column due to dead plus live loads from upper stories was applied as nodal loads at the column top. This axial load was applied as a ramp function over a period of 0.5 s as shown in Fig. 6.

Different charge weights of 100, 200, 500 and 1000 kg equivalent weight of TNT at stand-off distances of 1, 4 and 15 m were considered in the study. Both the un-strengthened and CFRP- strengthened columns were subjected to these blast loads. The blast loads impinging on the contact segments of the column were calculated by the software using ConWep [25]. The contact segments of the blast were the solid elements of the front face of the column which were taken to be in contact with the blast. The vertical height of the charge was taken as 1.0 m above the base of the column because the explosive is assumed to be carried in a vehicle. Thus, the shock transmitted to the column through ground gets diminished due to which it has been ignored in the analysis. The blast loading was set to trigger at 0.5 seconds as shown in Fig. 6.

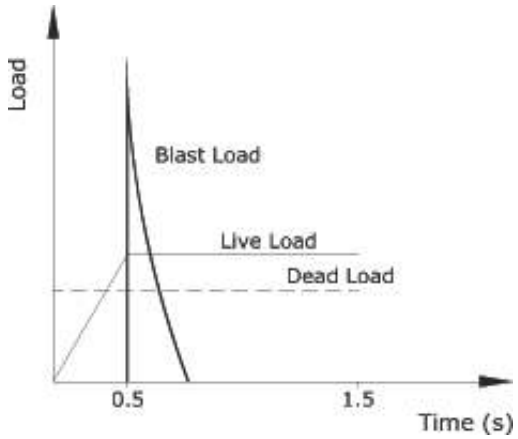

Figure 6 Loading procedure for dead, live and blast loads on column.

3.5 Solution strategy

LS-DYNA uses explicit time integration algorithm for solving the problems, which is less sensitive to machine precision than other finite element solution methods. The benefits of this are greatly improved utilization of memory and disk. An explicit FE analysis solves the incremental procedure and updates the stiffness matrix at the end of each increment of load (or displacement) based on changes in geometry and material. The termination time of 1.5 s was set in order to realize the complete blast related response of the column.

3.6 Blast load

The reflected pressure and positive phase duration found from ConWep for different charge weights considered in the study are plotted in Fig. 7. ConWep calculates air blast parameters using the equations found in Ref. [13] which is based on the data from explosive tests using weights from less than 1kg to over 400,000 kg. It is found from the air blast parameters calculation that ConWep may not be used for the explosion of 500 and 1000 kg charge weights at 1m range. The minimum range for the applicability of ConWep for 500 and 1000 kg charge weights is found as 1.42 and 1.79 m respectively. It is due to this reason that the column has been analyzed for these charge weights (i.e. 500 and 1000 kg) at 2m range and found to have completely destroyed. Thus obviously these charge weights at 1 m range would also destroy the column. Though no analysis for these charge weights at 1 m range has been carried out but the results reported latter for these cases are based on the results of analysis for 2 m range.

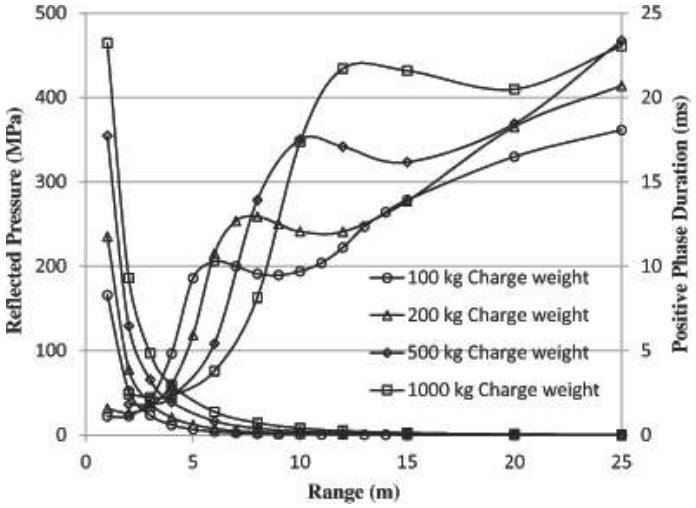

Figure 7 Reflected pressure and positive phase duration for different charge weights.

4 ANALYSIS RESULTS

4.1 Effect of mesh size

Two cases, one each from the un-retrofitted and the retrofitted column cases of blast scenarios were used to compare the results of the two meshes considered above for the purpose of mesh sensitivity analysis. Table 5 shows the results of the numerical convergence study. The numerical convergence study showed that further decrease in the mesh size has little effect on the numerical results but leads to the risk of computer memory overflow and substantially increases the computing time. In order to achieve maximum computing efficiency and thereby reduce the run-time, it was decided to use Mesh-1 for all parametric cases of blast loading simulation.

Table 5 Results of mesh sensitivity analysis.

Parameter	Column without FRP (200 kg charge at 4m standoff distance)		Column with FRP (1000 kg charge at 4m standoff distance)	
	Mesh 1	Mesh 2	Mesh 1	Mesh 2
Peak lateral displacement (mm)	41.05	43.23	124.98	123.40
Permanent lateral displacement (mm)	20.39	23.21	103.14	101.78
Max stresses in longitudinal bars (MPa)	512	508	623	606
Maximum stresses in transverse bars (MPa)	510	545	701	708

4.2 Displacements and time period of vibration

The time history of maximum lateral displacement of column for two typical combinations of charge weights and stand-off distances are shown in Figs. 8 and 9. The peak lateral and permanent displacement of column for the blast scenarios considered in the analysis are given in Table 6.

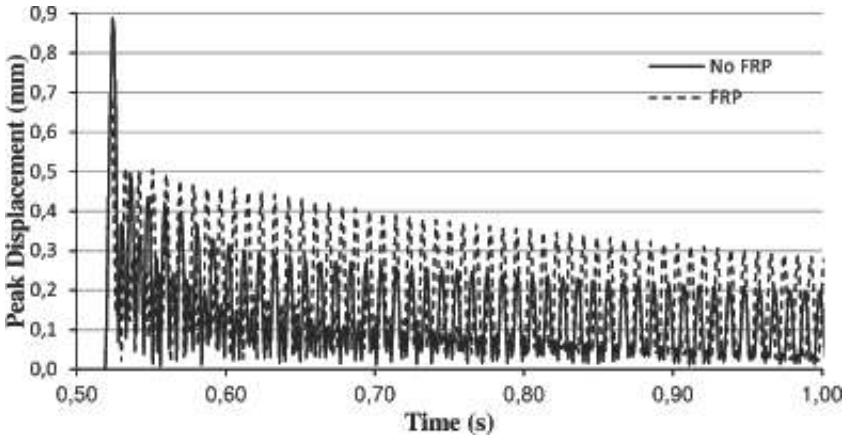

Figure 8 Lateral displacement of column subjected to blast due to 100kg charge at 15m stand-off distance.

The observations made from the displacement record are summarized below:

i) As stated previously, the charge weights of 500 and 1000 kg at a stand-off distance of 2.0 m completely destroyed both the columns with and without CFRP strengthening. Accordingly, these charge weights at 1 m range would also destroy the columns. So it can

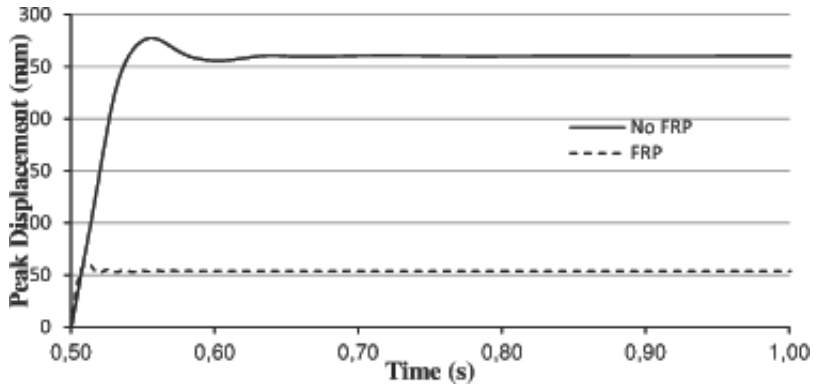

Figure 9 Lateral displacement of column subjected to blast due to 100kg charge at 1m stand-off distance.

be assumed that the columns within the focus of a blast of this magnitude would be totally destroyed and may not be protected by retrofitting.

ii) The retrofitted as well as un-retrofitted columns subjected to the blast of 100 kg charge weight at 15 m stand-off distance do not undergo any damage, thus the time period of vibration for this load case (Fig. 8) at the close of the period of analysis when the vibration is almost free should be the initial period of vibration of the column in the undamaged state. Thus the time period of the column initially in the undamaged state obtained from the free vibration response of column subjected to the least intensity blast (100 kg charge weight at 15 m stand-off distance) obtained from the end of the period of analysis is 10.2 and 9.0 s respectively for the un-retrofitted and retrofitted columns (Fig. 8). A comparison of these values with the analytically obtained time period (Table 3 and Fig. 4) shows that the values lie between the time period calculated for the first mode of the cracked and uncracked state with both ends fixed. This is due to the cracking of the column section due to vibration. The predominant mode of vibration initially is thus mode number 1 for both ends fixed condition.

iii) The retrofitting of column considered in the study results in 11.7% reduction in the initial natural time period of vibration of the column as obtained from the free vibration response of column subjected to the least intensity of blast (100 kg charge weight at 15 m stand-off distance) obtained from the end of the period of analysis.

iv) The retrofitting of column reduces the peak lateral displacement considerably. The retrofitting of column reduces the peak displacement by 21% when the damage to the column is almost negligible i.e. when the intensity of blast is least severe (100 kg charge weight at 15 m stand-off distance). A study of all blast cases considered indicates that the reduction of peak displacement varies from 8% for 100 kg charge weight at stand-off distance of 4 m to 79% for 500 kg charge weight at a stand-off distance of 4 m.

Table 6 Peak and permanent lateral displacement of column for different blast scenarios*.

Charge Weight (kg)	Peak displacement (mm)			Permanent displacement (mm)		
	d = 1 m	d = 4 m	d = 15 m	d = 1 m	d = 4 m	d = 15 m
Column without retrofitting						
100	277.53	10.54	0.89	260.21	3.95	0.08
200	489.53	41.05	1.83	478.89	20.39	0.10
500	∞	214.67	4.19	∞	173.55	0.53
1000	∞	474.85	8.39	∞	465.95	0.33
Retrofitted Column						
100	61.32	8.87	0.70	53.67	2.04	0.13
200	314.91	16.27	1.36	294.87	6.42	0.24
500	∞	45.00	3.50	∞	30.56	0.47
1000	∞	124.98	6.62	∞	103.14	0.61

*d: stand-off distance

v) There is exponential increase in peak lateral displacement as well as the permanent displacement with the reduction in the stand-off distance.

vi) At 15 m stand-off distance, the blast of even 1000 kg charge weight does not cause any significant damage to the column even without retrofitting. Considering 30 mm as the acceptable permanent lateral displacement for the column, at 4 m stand-off distance, blast of 100 kg charge weight may be resisted by the column even without retrofitting, whereas, 200 and 500 kg charge weights may be resisted by the column after retrofitting. Higher charge weight of 1000 kg could not be resisted by the retrofitting considered in the study. At a stand-off distance of 1 m, the blast of even 100 kg may not be resisted by even the retrofitted column. The increase in the number of layers of CFRP may however help the column to resist it.

vii) The time period of vibration gets elongated with cracking and damage to the column. The amount of damage (concrete fracture and yielding/fracture of steel) caused to the column increases with the increase in the intensity of blast, thus the time period of vibration also increases with increase in the charge weight and/or reduction in the stand-off distance (Figs. 8-9).

4.3 State of stress and consequent damage

Table 7 depicts the maximum tensile stress in the longitudinal as well as the transverse reinforcement bars as a result of different blast scenarios for both the retrofitted and the un-retrofitted columns. From the results in Table 7, it is noted that the maximum values of tensile stress for the transverse reinforcing bars in some blast scenarios for the retrofitted columns were found

to be higher than the corresponding blast scenarios of un-retrofitted columns. This is due to the erosion of concrete in un-retrofitted column which results in the release of stress in ties because the stress in ties is mainly due to the presence of concrete; whereas, the retrofitted column concrete being confined concrete, erosion is less and hence the stress in ties is more. For these cases it was also noticed that the un-retrofitted column had failed as a result of direct shear due to the proximity of the blast. However, the retrofitting of the columns for these cases improved the overall blast resisting capacity by increasing the shear capacity of the column.

Table 7 Maximum tensile stress in longitudinal and transverse reinforcement bars for different blast loading scenarios*.

Charge Weight (kg)	Maximum Tensile Stress longitudinal reinforcement (MPa)			Maximum Tensile Stress transverse reinforcement (MPa)		
	d = 1 m	d = 4 m	d = 15 m	d = 1 m	d = 4 m	d = 15 m
Column without retrofitting						
100	591	473	119	497	510	8.4
200	665	512	193	638	510	40
500	F	577	294	F	515	222
1000	F	620	443	F	508	502
Retrofitted column						
100	502	417	88	667	477	15
200	726	492	138	700	502	38
500	F	516	246	F	518	127
1000	F	623	367	F	701	384

*d = standoff distance; F = Failed

Tables 8 to 13 report the results of analysis for some of the critical cases of blast for column with and without CFRP strengthening. The results of analysis for 15 m stand-off distance have not been reported in these tables because of almost insignificant damage to the column. In addition, the results of 500 and 1000 kg explosive at 1.0 m stand-off distance have not been listed as the column (with and without CFRP strengthening) has been assumed to be completely destroyed as discussed earlier in Sec. 3.6 and 4.2. The final deflected shapes of the columns are also included in these tables. As seen from these tables, it is clear that the displacement experienced by the retrofitted columns is much lower compared with the un-strengthened columns. This demonstrates that CFRP strengthening might be a valuable tool in protecting the service integrity of RC columns especially when the blast charge weights are smaller.

Table 8 Damage of column due to 100 kg charge weight at 1 m stand-off distance.

Column status	Damage description
	Column without retrofitting
	**Lateral displacement**: The column was found to have a maximum lateral peak deflection of 277 mm. **Concrete:** Concrete was completely destroyed over the bottom one-third height. Severe dilation of concrete at mid-height and slight dilation near the top support of the column. The column rendered inadequate for service. **Longitudinal reinforcement:** No breakages were found in the bars. Max. tensile stress in the bars was 591 MPa. **Shear reinforcement**: No breakages in the ties were found. Max. tensile stress of 497 MPa was observed suggesting yielding of the bars.
	Retrofitted column
With FRP 	**Lateral displacement**: A maximum peak lateral deflection of 61 mm was observed. **Concrete:** Damage to concrete was seen at the bottom 0.5 m height of the column. The FRP material protected the concrete from any severe damage. **FRP material:** Partial tear of the FRP material was noticed at the bottom 1 m height of the column, on the side facing the blast wave and on the opposite face. **Longitudinal reinforcement:** There was no breakage in the steel bars but many bars were bent. Max. tensile stress of 502 MPa was observed suggesting yielding. **Shear reinforcement:** No breakages were observed in the ties. Tensile force data suggests some of the bars might have yielded. Overall the column might need some repairs for bringing it back to service life. Max. Tensile stress = 667 MPa

Table 9 Damage of column due to 100 kg charge weight at 4 m stand-off distance.

Column status	Damage description
	Column without retrofitting
	**Lateral displacement**: A small lateral deflection of 10 mm was observed. **Concrete:** Minor dilation of concrete at the bottom half meter height. Column seems to be in good service condition. **Longitudinal reinforcement:** Some of the bars were found to be slightly bent without any breakages. Max. tensile stress of 473 MPa was found. **Shear reinforcement:** Max. tensile stress of 510 MPa was found suggesting that the tie bars maybe close to yielding. However no breakages were found in the tie bars.
	Retrofitted column
	**Lateral displacement**: The lateral deflection of the column remains negligible (8 mm) in this case suggesting good serviceable condition of the column after the blast. **Concrete:** No damage to concrete core or cover was observed. **FRP material:** Very slight distortion in the material was seen in the top and bottom ends of the column. **Longitudinal reinforcement:** No breakages were seen in the longitudinal bars, only some of the bars were found to be bent. Max. tensile stress of 417 MPa was found in the bars. **Shear reinforcement:** No breakages in the tie bars were observed. Max. tensile stress of 477 MPa was observed suggesting only a few bars might be close to yielding.

Table 10 Damage of column due to 200 kg charge weight at 1 m stand-off distance.

Column status	Damage description
	Column without retrofitting
	**Lateral displacement**: Peak lateral deflection of 489 mm was found in the column. **Concrete:** Concrete in the bottom half was totally destroyed. The rest of the concrete was severely dilated leaving the entire column inadequate for service. **Longitudinal reinforcement:** Bars were found to have severely deformed. No breakages were detected. A maximum stress of 665 MPa was found in the bars, suggesting definite yielding of bars. **Shear reinforcement:** Tie bars were also severely bent. Max. stress of 638 MPa was found.
	Retrofitted column
	**Lateral displacement**: A peak lateral deflection of 314 mm was found. **Concrete:** Concrete over the bottom third height was critically damaged, however held together by the FRP. Spalling was also observed at the top end of the column. The column might have been rendered unfit for use. **FRP material:** Extreme damage and tearing was noticed at the bottom one-third height, and partial tearing at the top most part of the column. **Longitudinal reinforcement:** Bars badly bent out of shape at the blast height, and some of the bars were fractured at the top and the bottom ends of the column. Max. Tensile Stress = 726 MPa. **Shear reinforcement:** A few tie bars were found to have fractured at the bottom 1m height of the column. Max. Tensile Stress = 700 MPa.

Table 11 Damage of column due to 200 kg charge weight at 4 m stand-off distance.

Column status	Damage description
	Column without retrofitting
	**Lateral displacement**: Maximum Lateral deflection in the column was found to be approximately 41 mm. **Concrete:** Dilation of concrete was found especially in the bottom one-third height of the column. Minor dilation was found over the entire length. Column might be good for service loads after some repairs. **Longitudinal reinforcement:** No breakages in the bars, however the steel cage was bent at the bottom one meter height. Max stress of 512 MPa for observed. **Shear reinforcement:** No ties were broken. Some of them were slightly bent. Max. tensile stress = 510 MPa.
	Retrofitted column
	**Lateral displacement**: Overall the column seems to be in a good condition with a peak deflection of 16 mm. **Concrete:** No major damage. Slight dilation of concrete was noticed at the top end of the column as well as on the blast face in bottom 1 m height. **FRP material:** Slight distortion of the material was noticed in the bottom 1m height of the column on the blast face of the material. No tearing of the material. **Longitudinal reinforcement:** Bars were found to be bent at numerous locations, however no breakages were found. Max. tensile stress was 492 MPa, suggesting yielding in some of the bars. **Shear reinforcement:** Slight bending in some of the bars at mid-height, but no breakage. Max. tensile stress of 502 MPa suggesting some of the bars might be close to yielding.

Table 12 Damage of column due to 500 kg charge weight at 4 m stand-off distance.

Column status	Damage description
	Column without retrofitting
	**Lateral displacement**: The deflection (215 mm) in the column might render it unable to go on in service without major repairs. **Concrete:** Considerable lateral deflection in the column was found at mid-height as seen in the figure. Severe dilation in the concrete over the entire length of the column. **Longitudinal reinforcement:** The steel cage was also found to be considerably bent. However no breakages were detected. Max. tensile stress of 577 MPa suggesting yielding of bars. **Shear reinforcement:** Ties were found to be bent at a few locations. No breakages found. The axial force in the tie bars suggested definite yielding of bars. Max. tensile stress of 515 MPa.
	Retrofitted column
	**Lateral displacement**: It was found that the column had deflected at 1 m height by 45 mm. **Concrete:** Damage compared with the column without FRP got reduced. However no spalling of cover was found and the concrete core was intact. **FRP material:** The distortion of FRP material was more at the top and the bottom third heights of the column suggesting severe strain on the material at those locations. However no tearing of material was noticed. **Longitudinal reinforcement:** Slight deflection was found in the entire steel cage suggesting the column also had deflected to an extent. Max. tensile stress = 516 MPa. **Shear reinforcement:** Tie bars had no breakages; however some of them were bent. Max. axial stress of 518 MPa was observed suggesting some of the bars had just yielded.

Table 13 Damage of column due to 1000 kg charge weight at 4 m stand-off distance.

Column status	Damage description
	Column without retrofitting
	**Lateral displacement**: The column might have been rendered unusable as a result of a max. peak lateral deflection of 475 mm. **Concrete:** Severe concrete spalling found at a height of 0.5m above base. Damage to concrete at the bottom half of the column. Severe dilation over the entire height of the column. **Longitudinal reinforcement:** Bars were found to be deflected. No breakages were found however. Max. axial stress of 620 MPa was found suggesting bars have almost reached their tensile strength. **Shear reinforcement:** Ties were also found to be severely bent at more than a few locations. Tensile stress of 508 MPa suggest definite yielding of some of the bars.
	Retrofitted column
	**Lateral displacement**: A max lateral displacement of 125 mm was observed at the 1 m height of the column. **Concrete:** Dilation of concrete was found over the entire length. Concrete cover had spalled up to the bottom 1m height on the side facing the blast. However concrete core was found to be intact. **FRP material:** FRP material had torn up to the bottom 1m height and at the top end as shown in the figure. **Longitudinal reinforcement:** The steel bars were found to be bent at some locations, however no breakage was found. Max. tensile stress of 616 MPa was found suggesting yielding. **Shear reinforcement**: The steel tie bars were cut at four locations at the bottom third height specifically where the blast took place. Major repairs might be needed for the column in order to restore its service state. Max. tensile stress = 700 MPa

5 CONCLUSIONS

The major conclusions derived from the present study of un-retrofitted RC column and the lightly retrofitted column using CFRP are given in the following:

i) The frequency/time period of vibration of circular column obtained analytically is found to be close to the initial frequency/time period obtained through finite element analysis. The retrofitting of column considered in the study results in 11.7% reduction in the initial natural time period of vibration of the column.

ii) The retrofitting of column reduces the peak lateral displacement considerably, which varies from 8% for 100 kg charge weight at stand-off distance of 4 m to 79% for 500 kg charge weight at a stand-off distance of 4 m.

iii) There is exponential increase in peak lateral displacement as well as the permanent displacement with the reduction in the stand-off distance. Thus, the stand-off distance plays a very important role in mitigating the adverse effects of a blast.

iv) The charge weights of 200 and 500 kg at 4 m stand-off distance may be resisted by the column after retrofitting. However, the increase in the number of layers of CFRP may help the column to resist even slightly more intense blasts.

v) The time period of vibration gets elongated with the amount of damage (concrete fracture and yielding/fracture of steel) caused to the column; thus, the time period of vibration increases with increase in the charge weight and/or reduction in the stand-off distance.

vi) A comparison of the retrofitted RC column with un-retrofitted column cases reveals that even a light retrofitting considered in the study provided considerable resistance to blast loads, and thus contributed greatly to impeding the onset of progressive collapse for moderate blasts. The nature of the failure for CFRP-wrapped columns was also less explosive, thereby protecting loss of human life and property.

Acknowledgements: The authors gratefully acknowledge the support provided by the Specialty Units for Safety and Preservation of Structures and the MMB Chair of Research and Studies in Strengthening and Rehabilitation of Structures, Department of Civil Engineering, King Saud University.

References

[1] S.H. Alsayed, Y.A. Al-Salloum, T.H. Almusallam, and N.A. Siddiqui. Seismic response of FRP-upgraded exterior RC beam-column joints. *Journal of Composites for Construction ASCE*, 14(2):195–208, 2010.

[2] S.H. Alsayed, T.H. Almusallam, Y.A. Al-Salloum, and N.A. Siddiqui. Seismic rehabilitation of corner RC beam-column joints using CFRP composites. *Journal of Composites for Construction ASCE*, 14(6):681–692, 2010.

[3] *ACI 318M-08: Building Code Requirements for Structural Concrete and Commentary*, 2008.

[4] X. Bao and B. Li. Residual strength of blast damaged reinforced concrete columns. *Int Journal of Impact Engineering*, 37(3):295–308, 2010.

[5] J-O. Berger, P.J. Heffernan, and R.G. Wight. Blast testing of CFRP and SRP strengthened RC columns. In N. Jones and C.A. Brebbia, editors, *Structures Under Shock and Impact X, The Built Environment*, volume 98. WIT Press, 2008. Transactions of the Wessex Institute.

[6] P.A. Buchan and J.F. Chen. Blast resistance of frp composites and polymer strengthened concrete and masonry structures – a state-of-the-art review. *Elsevier Journal of Composites Part B*, 38:509–522, 2007.

[7] F.K. Chang and K.Y. Chang. Post-failure analysis of bolted composite joints in tension or shear-out mode failure. *Journal of Composite Materials*, 21:809–823, 1987.

[8] A.K. Chopra. *Dynamics of Structures – Theory and Applications to Earthquake Engineering*. Pearson Prentice Hall, Upper Saddle River, New Jersey, 3rd edition, 2007.

[9] J.E. Crawford, L.J. Malwar, and K.B. Morrill. Reinforced concrete column retrofit methods for seismic and blast protection. In *Proc. of society of American military engineering symposium on compressive force protection*, Charleston, USA, 2001.

[10] J.E. Crawford, L.J. Malwar, K.B. Morrill, and J.M. Ferritto. Composite retrofits to increase the blast resistance of reinforced concrete buildings. In *Proc. of 10th Int. symp. on interaction of the effects of munitions with structures*, pages 1–13, San Diego, USA, 2001.

[11] J.E. Crawford, L.J. Malwar, J.W. Wesevich, J. Valancius, and A.D. Raynolds. Retrofit of reinforced concrete structures to resist blast effects. *ACI Structural Journal*, 94(4):371–377, 1997.

[12] K.W. King, J.H. Wawclawczyk, and C. Ozbey. Retrofit strategies to protect structures from blast loading. *Canadian Journal of Civil Engineering*, 36(8):1345–1355, 2009.

[13] C.N. Kingery and G. Bulmash. Airblast parameters from TNT spherical air burst and hemispherical surface burst. Technical Report ARBL-TR-02555, United States Army BRL, 1984.

[14] S. Lan, J.E. Crawford, and K.B. Morrill. Design of reinforced concrete columns to resist the effects of suitcase bombs. In *Proc. of 6th Int. conf. on Shock and Impact Loads on Structures*, pages 5–10, Australia, 2005. Perth.

[15] *LS-DYNA User's Keyword Manual, Ver. 971*, 2007.

[16] A. Malhotra, D. Carson, and T. Stevens. Demystifying blast effects on buildings – I. In *Proc. of First International Workshop on Performance, Protection, and Strengthening of Structures under Extreme Loading*, Whistler, Canada, 2007.

[17] L.J. Malvar, J.E. Crawford, and K.B. Morrill. *K&C concrete material model Release III – Automated generation of material input*, 2000. K&C Technical report TR-99-24-B1.

[18] A. Matzenmiller and J.K. Schweizerhof. Crashworthiness considerations of composite structures – a first step with explicit time integration in nonlinear computational mechanics – state-of-the-art. Springer Verlay, 1991.

[19] K.B. Morrill, L.J. Malwar, J.E. Crawford, and J.M. Ferritto. Blast resistant design and retrofit of reinforced concrete columns and walls. In *Proc of structures congress- building on the past- securing the future*, Nashville, TN, USA, 2004.

[20] L.C. Muszynski and M.R. Purcell. Composite reinforcement to strengthen existing concrete structures against air blast. *Journal of Composites for Construction*, 7(2):93–97, 2003.

[21] L.C. Muszynski, M.R. Purcell, and R. Sierakowski. Strengthening concrete structures by using externally applied composite reinforcing material. In *Proc. of 7th Int. symp. on interaction of the effects of munitions with structures*, pages 291–298, Germany, 1995.

[22] B. Riisgaard, A. Gupta, P. Mendis, and T. Ngo. Finite element analysis of polymer reinforced CRC columns under close-in detonation. In *Proc of 6th European LS-DYNA User's Conference*, Gothenburg, Sweden, 2007.

[23] Y. Shi, H. Hao, and Z-X Li. Numerical derivation of pressure–impulse diagrams for prediction of RC column damage to blast loads. *Int. Journal of Impact Engineering*, 35(11):1213–1227, 2008.

[24] Y. Shi, Z-X. Li, and H. Hao. Bond slip modelling and its effect on numerical analysis of blast-induced responses of RC columns. *Structural Engineering and Mechanics*, 32(2):251–267, 2009.

[25] Conwep. conventional weapons effects. Computer software produced by U.S. army Waterways Experimental station, 1990. Mississippi, USA.

[26] W.F. Mekky W.W. El-Dakhakhni and S.H. Changiz-Rezaei. Vulnerability screening and capacity assessment of reinforced concrete columns subjected to blast. *J. Perf. Constr. Fac*, 23(5):353–365, 2009.